Shahrood University of Technology
Iranian Society of Mining Engineering (IRSME)
Journal of Mining and Environment (JME)
journal homepage: www.jme.shahroodut.ac.ir
THOMSON REUTERS

Characterization of Micro-Structural Changes of Mechanically-Activated Ilmenite

Hussein Ebadi[1], Parviz Pourghahramani[1*] and Behzad Nemati Akhgar[2]

1. Mining Engineering Department, Engineering Faculty, Sahand University of Technology, Tabriz, Iran
2.Mining Engineering Department, Engineering Faculty, Urmia University, Urmia, Iran

Article Info

Received 14 April 2021
Received in Revised form 29 May 2021
Accepted 4 June 2021
Published online 4 June 2021

DOI:10.22044/jme.2021.10720.2033

Keywords

Ilmenite
Mechanical activation
Structural changes
XRD line profile analysis
Reactivity

Abstract

Structural changes of mechanically-activated ilmenite during milling by a planetary mill are monitored and determined as a function of the milling time. The maximum specific BET surface area of 10.76 m2/g is obtained after 150 min of milling. The results obtained indicate that agglomeration of the particles occurs after 45 min of milling. The maximum X-ray amorphization degree of ca. 95% has been calculated after 150 min of milling. Estimation of the stored energy reveals that the X-ray amorphization degree has a dominant contribution to the excess enthalpy of the activated materials. The surface-weighted crystallite size in the ground ilmenite reaches 4.45 nm, which corresponds to the volume-weighted crystallite size of 8 nm and 11.18 nm obtained by the Williamson-Hall and Rietveld methods, respectively. After 150 min of mechanical activation, the root mean square strain, , increases to 0.78%, which corresponds to the strains of 1.43% and 1.04% obtained from the Williamson-Hall and Rietveld methods, respectively. Reduction in the crystallite size leads to the contraction of the ilmenite unit cell after 150 min. The reaction rate constant of the ilmenite dissolution increases by over 58 times after 150 min of milling. Activation energy of the dissolution reaction decreases from 57.45 kJ/mol to 41.09 kJ/mol after 150 min of milling.

1. Introduction

Mechanical activation refers to a process wherein large amounts of energy are mechanically transferred to the materials during a high-energy milling, whereas the chemical composition of the materials involved remains unchanged (Lin I, 1998) [1]. As a result, after mechanical activation, these materials possess a high entropy, a high free energy, and a high tendency to contribute to a reaction (Baláž, 2000, Boldyrev and Tkáčová, 2000, Tkáčová, 1989) [2-4]. It is well-known that mechanical activation is useful to increase the reactivity of minerals during the leaching process, sintering, smelting, and production of nano-minerals with special properties (Baláž, 2000) [2].

The micro-structural changes and phase transformation of mechanically-activated ilmenite has been studied for different cases. The results obtained for the micro-structural changes and phase transformation during the mechanical activation are different. Welham and Llewellyn (1998) [5] have reported that as ilmenite is mechanically activated in a conventional ball mill for more than 100 h, the crystallite size decreases and the lattice strain increases without any detectable phase transformation. On the other hand, Chen (1999) [6] has reported a gradual conversion of ilmenite to pseudo-rutile ($Fe_2Ti_3O_9$) during mechanical activation under the air atmosphere after 200 h of milling by a planetary ball mill. Previous investigations have generally focused on the study of the effects of mechanical activation in different milling conditions on the dissolution rate of ilmenite during leaching by sulfuric or hydrochloric acid (Welham and Llewellyn, 1998, Chen. Williams, Campbell and Wang 1999, Li, Liang, Guo and Wu, 2006, Li,

Corresponding author: Pourghahramani@sut.ac.ir (P, Pourghahramani).

Liang and Wang, 2008, Sasikumar, Rao, Mukhopadhyay, and Mehrotra, 2007, Sasikumar, Rao, Srikanth, Ravikumar, Mukhopadhyay and Mehrotra, 2004, Zhang, Hu, Wei, Chen, and Tan, 2010, Zhang, Hu, Wei, Chen and Tan, 2010) [5-12]. The results obtained have revealed that an intensive milling process increases the dissolution rate of ilmenite. A detailed literature survey indicates that the milling of ilmenite concentrate produces a nano-crystalline structure with different levels of micro-strain. The difference in the results could be attributed to different milling conditions, various ilmenite sources, and using unsophisticated microstructural characterization approaches that lead to large errors in the calculation steps of micro-structural characteristics. Unfortunately, to the best of our knowledge, the micro-structural changes of ilmenite during mechanical activation have not been studied exclusively using the professional methods of micro-structural analysis. In addition, in the conducted studies, calculation of some important parameters such as the X-ray amorphization degree have been ignored, whereas the X-ray amorphization degree is considered as the most important micro-structural parameter regarding the atomic bonds strength. It is well-known that more than 90% of the energy stored in the structure of mechanically activated materials relates to the amorphization (Pourghahramani and Forssberg, 2006) [13]. As a result, the underlying factors behind the changes in the reactivity of the mechanically activated ilmenite could not be fairly comprehended because the changes in the reactivity of the mechanically activated materials during the steps of a process depend largely on the available structural characteristics at each step of the process (Pourghahramani and Azami, 2015, Senna, 1989) [14, 15], an exact structural refinement approach, and the data collection before making any interpretation is of prime importance.

In this work, the micro-structural changes and reactivity of the Iranian ilmenite concentrate during milling by a high-energy planetary ball mill were investigated using the X-ray diffraction line profile analysis. The Williamson-Hall (W-H), Warren-Averbach (W-A), and Rietveld methods were used for a precise determination of the crystallite size and lattice strain. In the following, the dislocation density, change in the lattice volume, and stored energy were calculated for the mechanically-activated ilmenite. In addition, an insight into the reactivity of mechanically-activated ilmenite concentrate in the initial process of TiO_2 pigment production was elucidated.

2. Experimental

2.1. Materials

The Ghara-aghaj ilmenite concentrate from a polymetallic ore in Iran was selected for the mechanical activation experiments. The Ghara-aghaj titanium deposit is located 36 km from the North-West of Euromieh (Iran). The mineralogical study of the concentrate using an optical microscope indicates the presence of magnesium-hornblende in the concentrate. Analysis of the XRD patterns obtained (Figure 1) has revealed mainly the reflection peaks of $FeTiO_3$ corresponding to JCPDS No. 01-075-1210. The peak at $2\Theta = 28.7^{\circ}$ is related to magnesium-hornblende, which corresponds to JCPDS No. 00-045-1371. Chemical analysis of the ilmenite concentrate indicates that the concentrate comprises 45.50% of TiO_2 (Table 1).

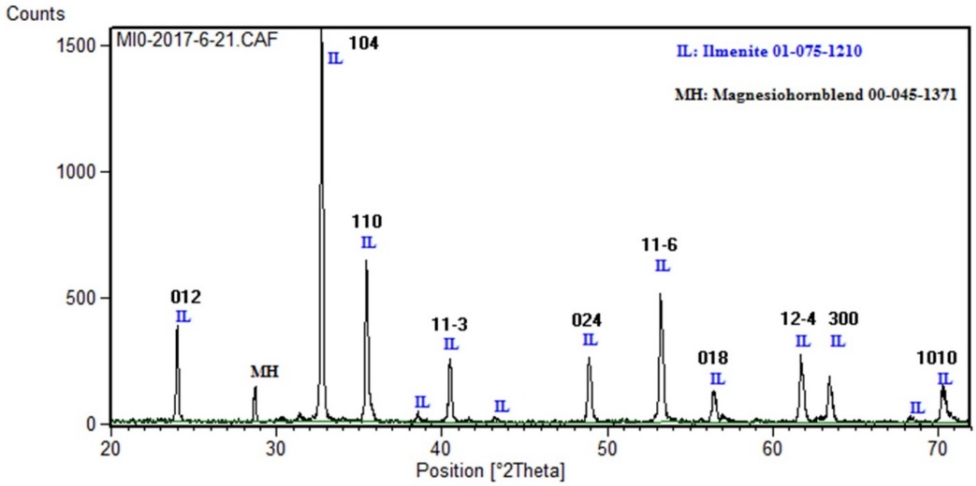

Figure 1. XRD pattern of the ilmenite concentrate.

Table 1. Chemical analysis of the Ghara-aghaj ilmenite concentrate.

Oxide	TiO_2	Fe_2O_3	SiO_2	Al_2O_3	CaO	MgO	MnO	P_2O_5	Cr_2O_3	Na_2O	LOI	Total
(Wt %)	45.22	50.21	3.43	0.35	0.37	2.32	0.88	0.12	0.02	0.2	-3.12	100

2.2. Characterization

Characterization of the samples were carried out using XRD, BET surface area measurements, laser particle size analysis, and SEM analysis. An X-ray powder diffractometer (Bruker Axs D8, Germany) was used to collect the XRD patterns using Cu Kα radiation (λ = 1.5406 Å) at 40 kV and 40 mA. For all records, the 2Θ range of 20–72°, step size of 0.02° and counting time of 3 s were used. The line profile analysis of the XRD patterns was carried out by the Winfit software (Krumm, 1996) [16] in order to extract the XRD line parameters. A laser diffraction instrument (Mastersizer 2000, Malvern, UK) was employed for the particle size analysis of the samples to measure the particle size distribution and granulometric surface area. The specific surface area of the activated and non-activated samples was measured by Belsorp mini II (Microtrac BEL Corp, Japan) using the BET method. Scanning electron microscopy (VEAGA-SEM TS5136MM, Czech Republic) in the backscatter electron imaging mode was used for the SEM characterization. Ultraviolet-visible spectroscopy (SPECORD 200, Germany) was used for the analysis of the Ti content in the leaching solution.

2.3. Mechanical activation

Planetary ball mill (Pulverisette 6, FRITSCH, Germany) was used for activation of the Ghara-aghaj ilmenite concentrate by applying a rotation speed of 450 rpm. Mechanical activation of the samples was carried out for 20, 45, 90, and 150 min and twelve stainless steel balls with a diameter of 19 mm with the ball to powder weight ratio of 15:1 were used in the milling process. In order to reduce the sticking of powder to the milling media and cup, milling was stopped at the given milling intervals, and the powders were softened. The powder samples obtained were sealed and kept in a freezer.

2.4. Dissolution tests

In order to assess the high-energy ball milling effect on the ilmenite reactivity, a series of dissolution tests were carried out using a 50% (w/w) sulfuric acid solution. A 250 mL three-necked flat-bottom flask equipped with a reflux condenser and a thermometer was used for the dissolution tests. In each experiment, 250 mL of the sulfuric acid solution was poured in the flask and heated by a hot plate in order to reach the desired temperature. Then 2.50 g of the ilmenite concentrate was added to the acid solution and stirred by a magnet stirrer.

2.5. Profile fitting

Profile fitting is the first step in the micro-structural characterization of X-ray diffraction pattern to extract the XRD line parameters. In profile fitting, firstly, the $K\alpha_2$ component of peak profile was removed, the $K\alpha_1$ intensity was double the $K\alpha_2$ intensity, and next, the profile backgrounds were subtracted and the overlapped peaks were resolved. The peaks (012), (104), (110), (11-3), (024), (11-6), (12-4), and (300) related to the ilmenite diffraction were used for characterization of the ilmenite micro-structural changes by the line profile analysis method. The XRD line profiles of the activated, non-activated, and standard LaB_6 samples were fitted by a combination of the Gaussian and Cauchy functions. A typical profile fitting to the XRD pattern is shown in Figure 2.

2.6. Micro-structural characterization

Any imperfection in the crystal structure causes changes in the XRD pattern background, peaks position, diffraction peaks intensity, and broadness of diffraction peaks. Broadness of a peak is related to the lattice strain and crystallite size, and these parameters can be calculated by the W-H equation, as bellow:

$$\beta_{hkl}\cos\theta_{hkl} = \frac{K\lambda}{D_v} + 4\varepsilon\sin\theta_{hkl} \quad (1)$$

where β_{hkl} is the physical broadening of the peak, θ is the Bragg angle of the (h k l) peak, λ is the wavelength of X-rays used, D_v is the crystallite size, ε is the lattice strain, and K is a constant. A more detailed information about k has been given by Langford and Wilson (1978) [17]. The intercept and slop of the plot of $\beta_{hkl}\cos\Theta_{hkl}$ as a function of $4\varepsilon\sin\Theta_{hkl}$ (W-H plot) are used for calculation of the lattice strain and domain size, respectively.

The W-A analysis is based on the measurement of the structural broadening of two (or more) reflection peaks from the same crystallographic planes. The W-A method separates the effect of

crystallite size and root mean square strain (RMSS) by fitting the Fourier series to the peak profiles. A detailed explanation of the approach has been given in our previous study (Pourghahramani and Forssberg, 2006) [18]. A more detailed information about the W-A method has been given by Warren (1969) [19] and summarized by Bourniquel *et al.* (1989) [20].

Rietveld analysis is another practical method for the micro-structural characterization of the materials. Principles of the Rietveld analysis have been presented by H.M. Rietveld (1969) [21]. This method uses the crystallographic data for simulating the X-ray diffraction pattern via a full profile fitting of a measured XRD pattern. The fitting goodness is measured by Eguation (2) (Young, 1993) [22].

$$R = \sum_i W_i \left[y_i \left(obs \right) - y_i \left(calc \right) \right]^2 \qquad (2)$$

where y_i *(obs)* is the observation intensity, y_i *(calc)* is the calculated intensity, and W_i is a coefficient that equals to $1/y_i(obs)$. The R values for the analysis in the present work were obtained to be less than 10 and close to 1, which signified a good fit.

The X'Pert High Score Plus software (Degen, Bron, König and Nénert, 2014) [23] was used for the Rietveld analysis in this work. A typical profile fitting by the Rietveld method on a XRD pattern of mechanically-activated ilmenite is shown in Figure 3.

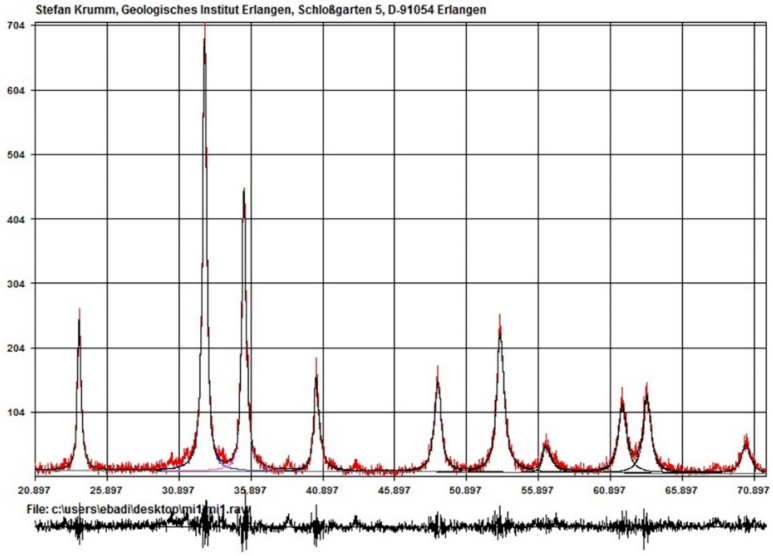

Figure 2. A typical profile fitting of XRD diffraction pattern for 20 min mechanically-activated ilmenite. The observed and measured patterns and their differences are pictured.

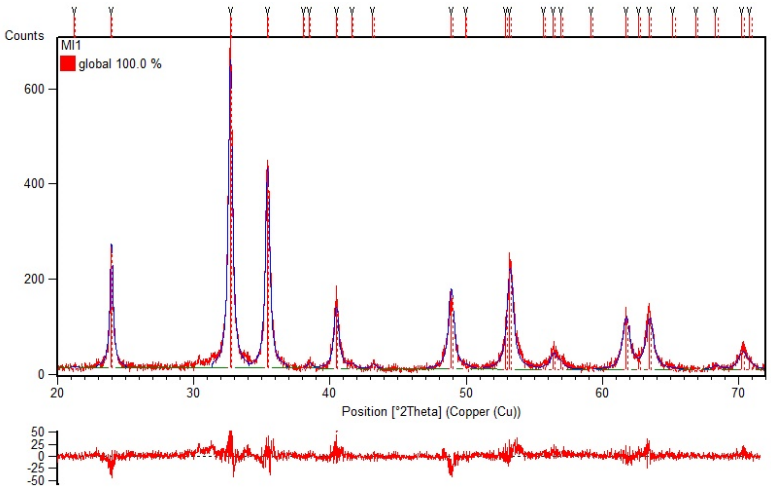

Figure 3. Rietveld analysis of the activated ilmenite. The measured profile (red line) and the calculated profile (blue line) are shown in the figure.

3. Results and Discussion

3.1. Size distribution and morphology of particles

The granulometric and BET specific surface areas are the main characteristic parameters that are subjected to a significant change during the mechanical activation. The results obtained, shown in Figure 4, emphasize on the variations. The BET surface area increases with the milling time up to 16 times, and in the final stage, reaches the maximum value of 10.76 m^2/g. The granulometric surface area increases rapidly from 0.55 m^2/g for the un-milled ilmenite concentrate to 5.85 m^2/g after 20 min of milling. However, by extending the milling, its value falls to 4.26 m^2/g after 90 min milling and increases again to 6.53 m^2/g in the 150 min milled sample. The simultaneous decrease in the granulometric surface area and increase in the BET surface area implies the agglomeration of the particles. These agglomerated particles are porous and accessible for nitrogen gas in the BET analysis, so the BET specific surface area increases as the granulometric surface area decreases. The particle size distributions are compared in Figure 5. It is clear that the activated sample for 20 min yields the finest product. A prolonged milling led to the re-welding and agglomeration of the particles, and a further size reduction was impossible. The agglomeration phenomenon causes the particles size distributions from prolonged milling to move toward larger sizes. It could be expected that the agglomeration continues with the extended milling. Similar results have been reported in the previous investigations for hematite activated in a vibratory mill (Pourghahramani and Forssberg, 2006) [18], for pyrite activated in a planetary mill (Pourghahramani and Akhgar, 2015) [24], and for olivine activated in a Spex mill (Li and Hitch, 2016) [25] suggesting that agglomeration is a probable phenomenon in the dry milling process.

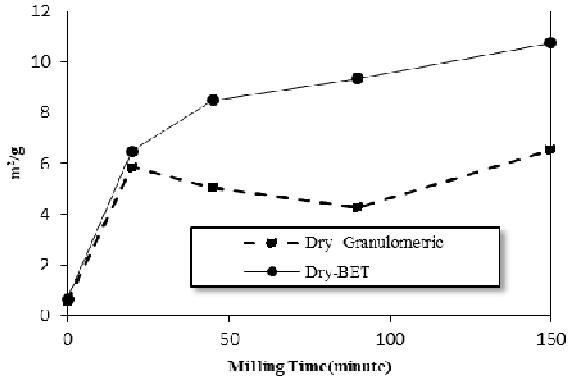

Figure 4. BET and granulometric surface area variations with the milling time.

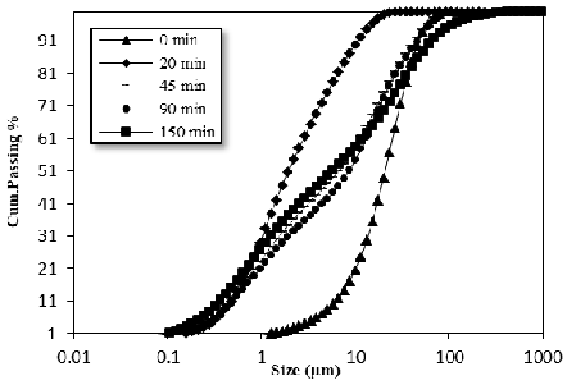

Figure 5. Particle size distributions of the un-milled and mechanically activated ilmenites.

SEM images of the un-milled and milled ilmenite concentrates are shown in Figure 6 Un-milled particles are completely angular with fractured surfaces. It can be seen that with the formation of strong clusters, agglomeration occurs by prolonged milling. It is clear that the agglomerated particles are dense in the initial stage of milling (45 min, a and b); by extending the milling time, the particles were ground again, and the agglomerated flaky particles with a low density were produced. The results obtained are in agreement with the surface area measurements and particle size distributions.

3.2. X-ray diffraction

XRD profiles of the activated and non-activated ilmenite samples are represented in Figure 7. All the patterns indicate a hexagonal structure of the ilmenite phase, matching the standard XRD pattern of the hexagonal structure $FeTiO_3$. The peak related to the magnesium-hornblende mineral ($2\Theta = 28.7^{\circ}$) disappeared after 20 min of milling. XRD analysis did not reveal any new crystalline phase formation. Based on the report of Sasikumar et al. (2004) [10], the traces of pseudo-rutile cannot be detected in the XRD patterns due to amorphization. There is no evidence for the formation of pseudo-rutile in the XRD pattern obtained. On the other hand, from the macroscopic visualization, it was found that the color of the milled samples for 90 and 150 min was different from the un-milled ilmenite. The changes in the powder color is probably due to the surface oxidation of ilmenite, as cited before, ilmenite milling in air leads to oxidation (Chen, Williams, Campbell and Wang, 1999) [6]. Li et al. (2006) [7] have provided more evidence by TG analysis as a portion of the Fe atoms of the activated ilmenite is oxidized during the mechanical activation.

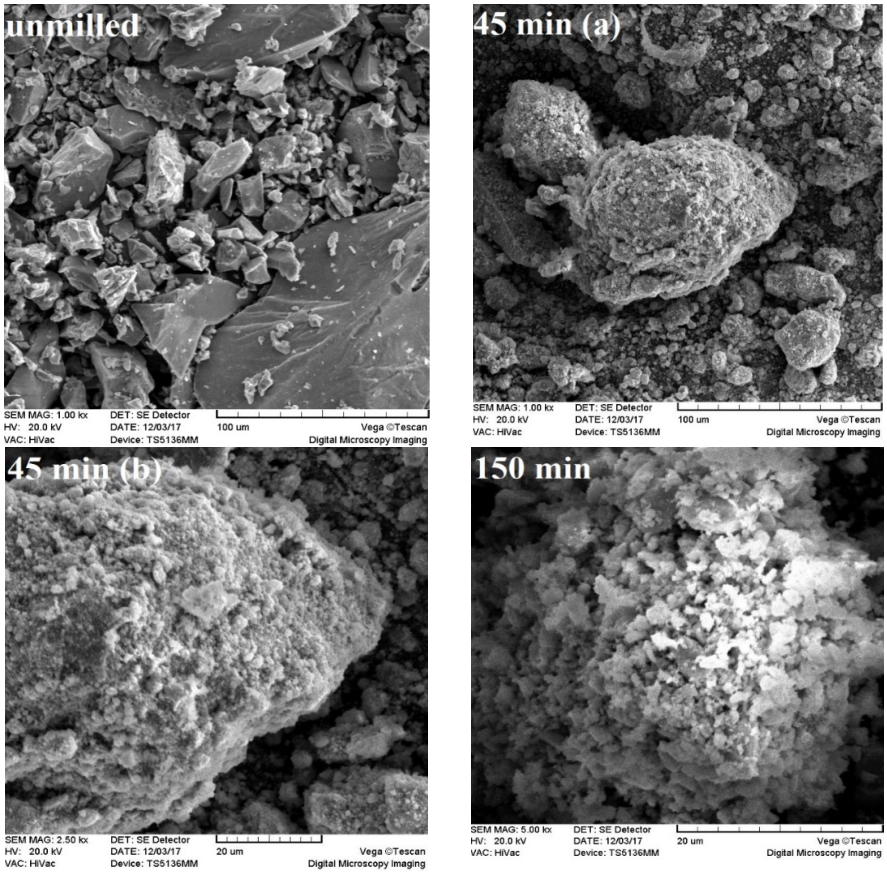

Figure 6. SEM images of un-milled and milled ilmenite for different times and magnifications.

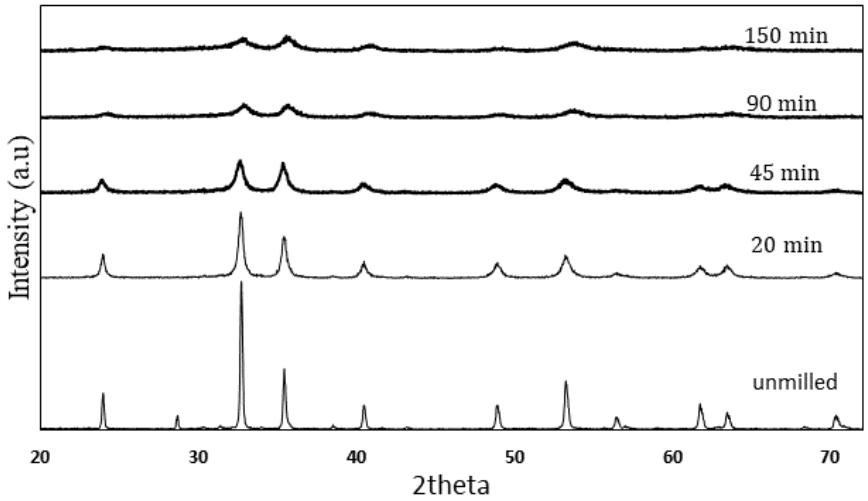

Figure 7. XRD patterns of the un-milled and mechanically-activated ilmenite for different milling times.

Mechanical activation of the ilmenite concentrate results in peaks broadening, changes in peak position, and decreases in the peaks intensity (Figure 8). Disordering of the material structure due to of the formation of the amorphous material is revealed by a decrease in the integral intensity of the diffraction lines. The broadening of the diffraction peaks is due to the plastic deformation and breakdown of the particles as it is obvious with increasing mechanical activation time. In the case of a prolonged milling time, these changes are more significant. Figure 8 shows that the

diffraction peaks of ilmenite almost disappear after 150 min of mechanical activation. Compared with the results of other research works (Welham and Llewellyn, 1998, Li, Liang, Guo and Wu, 2006, Li, Liang and Wang, 2008, Sasikumar, Rao, Mukhopadhyay, and Mehrotra, 2007, Sasikumar, Rao, Srikanth, Ravikumar, Mukhopadhyay and Mehrotra, 2004, Zhang, Hu, Wei, Chen, and Tan, 2010) [5, 7-11], it appears that the changes in the micro-structural parameters of mechanically-activated ilmenite could be more intensive in this work due to the intensive treatment conditions.

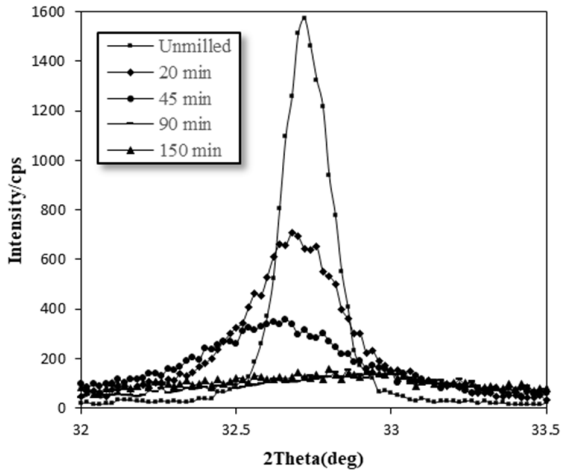

Figure 8. Variation in peak broadening, 2theta and intensity of main peak (104) of un-milled and mechanically-activated ilmenite.

3.3. Micro-structure characterization

The micro-structure characterization of the ilmenite concentrate and mechanically-activated samples were carried out by the W-H, W-A, and Rietveld methods. The Williamson-Hall plots were depicted using Eguation (1), and the results obtained were illustrated in Figure 9. The volume weighted crystallite size (D_v) and lattice strain were calculated using the Williamson-Hall plots. With increase in the milling time, the slope and intercept of the plots increase continuously but at the milling times more than 90 min, the slope of plots has approximately remained unchanged. From the results obtained, it can be concluded that the crystallite size decreases continuously and the lattice strain reaches the maximum value by 90 min, and then remains almost constant. The Rietveld and W-H results are in line with each other, implying the validity of the results obtained. The W-H method estimates a larger lattice strain in comparison with the Rietveld method. This trend has also been reported by Jiajie Li and Michael Hitch (2016) [25] for the mechanically-activated olivine.

In addition, the micro-structural characteristics were determined using W-A based on the Fourier transformation of the XRD lines, and the results obtained were compared in Table 2. It can be observed that the surface-weighted crystallite size in ground ilmenite is 4.45 nm after 150 min in the planetary mill, corresponding to a volume-weighted crystallite size of 8 nm. After 150 min mechanical activation, the root mean square strain, $< \varepsilon^2_{L=10nm} >^{1/2}$, increases to 0.78%, corresponding to the strain of 1.43% obtained from the W-H approach.

The results of the W-H and W-A methods must be in a limited range based on the line profile shape. If the broadened strain contains a Cauchy component, there will be no a clear correlation between *RMSS* and ε. Balzar (1999) [26] has presented a rough estimation as Eguation (3) when the Cauchy and Gauss extremes of the strain broaden the Voigt profile exist:

$$0.5 \leq \frac{\varepsilon}{< \varepsilon_l^2 >^{\frac{1}{2}}} \leq 2 \qquad (3)$$

On the other hand, the relationship between D_v and D_s (surface-weighted crystallite size calculated from the W-A method) for a Voigt size-broadened profile are given by:

$$1.31 \leq \frac{D_v}{D_S} \leq 2 \qquad (4)$$

For other methods:

$$\frac{D_v}{D_S} \leq r \qquad , 1 \leq r \leq 3 \qquad (5)$$

In the present work, the value of Eguation (3) for the calculated strain results using the W-H and W-A methods varies in range of 1.26-1.84. Therefore, it could be concluded that the W-H and W-A method results are in good agreement with each other. In addition, D_v/D_s for the crystallite sizes is in the range of 1.44-2.67.

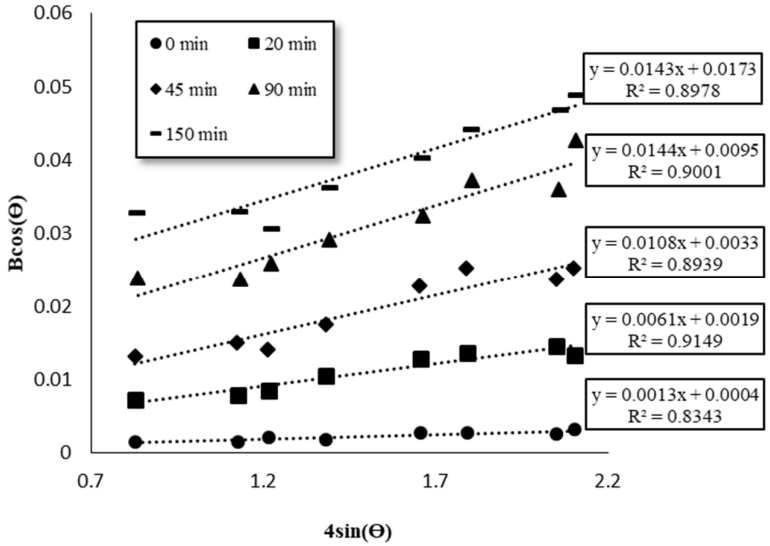

Figure 9. W-H plots for the ilmenite concentrate samples milled with different times.

Table 2. Microstrain and crystallite size measurement results of un-milled and mechanically-activated ilmenite samples.

Milling time (min)	W-H		W-A		Rietveld	
	D_v (nm)	ε (%)	D_s (nm)	RMSS (%)	Dv (nm)	ε (%)
0	346.63	0.13	239.60	0.10	183.00	0.08
20	72.98	0.61	43.15	0.39	70.28	0.35
45	42.02	1.08	19.60	0.85	37.20	0.65
90	14.60	1.44	5.45	0.78	17.10	0.97
150	8.01	1.43	4.45	0.78	11.18	1.04

3.4. Changes in lattice parameters

As indicated in Figure 8, milling of the ilmenite concentrate changes the peak positions. A change in the peak position (2θ) leads to an increase or a decrease in d-spacing (Suryanarayana, Norton, 1998) [27]. Figs. 10 and 11 show the variations in the unit cell volume and lattice parameters, respectively. These changes coincide with a variation in d-spacing. The unit cell software (Holland and Redfern, 1997) [28] was used in order to refine the lattice parameters of ilmenite by the regression diagnostics method in the hexagonal system. After 45 min of milling, the ilmenite lattice expands, and then by extending the milling time unit cell volume shrinks. The sequence of unit cell expansion and shrinkage could presumably be due to the formation of lattice vacancy at the beginning of activation, and then substitution of some atoms in the lattice vacancies (Schubert, 2015) [29]. However, another explanation for causes of lattice volume variations is related to the excess volume of the grain boundary and interface tension. These two phenomena are present on the boundary of crystallites, and could affect the lattice volume of the materials with a nanometer scale micro-structure (Kumar, Bakshi, Joardar, Parida, Raja and Singh, 2017, Qin, Nagase, Umakoshi, and Szpunar, 2007) [30, 31]. Based on the thermodynamic theories, the interface tension creates a compressive stress in the structure of the material, which is inversely correlated with the crystallite size (Qin, Nagase, Umakoshi, and Szpunar, 2007) [31]. The compressive stress will increase by decreasing the crystallite size. The interfacial stress can be calculated in terms of the grain boundary (GB) interfacial energy (Cammarata, and Sieradzki, 1994) [32]. The milling process and the change in the crystallite size lead to the creation of excess GB energy in the crystallites interfaces. Excess GB energy can be calculated using Eguation (6) (Nazarov, Romanov and Valiev, 1996) [33].

$$\gamma_{GB}^{Excess} = \frac{Gb^2\rho d}{12(1-\pi)}\ln\left(\frac{d}{b}\right) \quad (6)$$

where G, b, ρ, and d denote the shear modulus, burger vectors, dislocation density, and crystallite size, respectively. For the ilmenite mineral, G and b are 90 GPa and 0.5088 nm, respectively (Tromans and Meech, 2001) [34].

Disordered grain boundary in mechanically-activated materials possesses some vacancies, which increase the grain boundary volume by a so-called excess free volume (Wagner, 1992) [35]. The excess free volume (ΔV) is calculated using Eguation (7) (Chattopadhyay, Nambissan, Pabi, and Manna, 2001) [36].

$$\Delta V = \frac{\left(d + \frac{\xi}{2}\right)^2 - d^2}{d^2} \quad (7)$$

where ξ is the grain boundary thickness ($\approx 1nm$) and d is the crystallite size. This free volume creates stress fields in the crystallites, and the atoms can shift their positions slightly toward the vacancies. If the excess volume effect is greater than the excess GB energy, the lattice will expand; otherwise, the lattice will contract. In the present work, the excess volume and excess GB energy were calculated as shown in Figure 12. The final contraction of the ilmenite unit cell and unit cell parameters indicate that the role of excess GB energy is dominant in comparison to the effect of excess free volume.

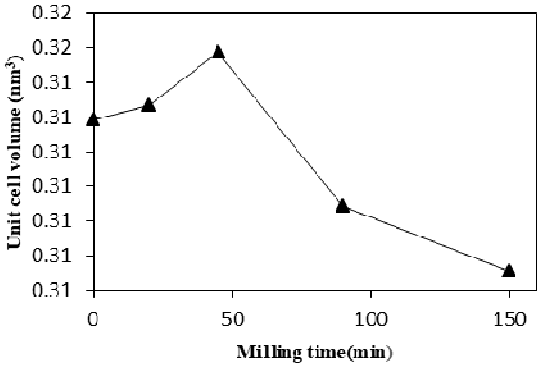

Figure 10. Changes in the unit cell volume of milled ilmenite.

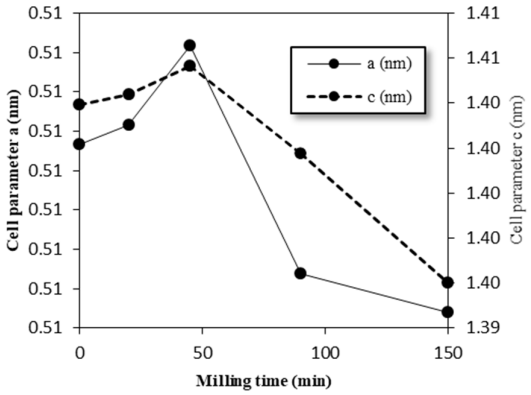

Figure 11. Changes in the unit cell parameters of milled ilmenite.

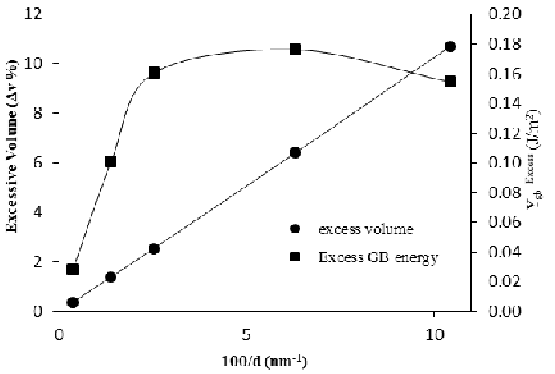

Figure 12. Variations in the excess free volume and excess GB energy versus crystallite size.

Calculation of the X-ray amorphization of the activated ilmenite was carried out using Eguation (1), as defined by Ohlberg and Strickler (1962) [37]:

$$A = 100 - X = 100 - \left(\frac{U_0}{I_0} \times \frac{I_x}{U_x} \times 100\right) \quad 1$$

In this formula, A is the X-ray amorphization, U_x and U_0 denote the background of the activated and non-activated samples, and I_x and I_0 refer to the integral intensities of the diffraction lines of the activated and non-activated samples, respectively. X is the degree of crystallinity. The term of X-ray amorphization degree refers to the change of long-range order of material structure to the short-range order due to intensive milling, which is not detectable by X-ray diffraction. Figure 13 depicts the X-ray amorphization degree of milled ilmenite and the relative intensity of peaks as a function of the milling time. The results obtained indicate that the ilmenite structure is rapidly disordered through high energy ball milling of ilmenite, whereas the amorphization degree increases to 66% in the intensive milled for 20 min. By extending the milling to 150 min, the amorphization degree is maximized at 95%.

3.5. Stored energy

Mechanical activation makes the structural changes in the surface and bulk of materials, and leads to an increase in the enthalpy of materials. This excess enthalpy is the stored energy in the particle surface (ΔH_s), grain boundary (ΔH_{GB}), elastic strain (ΔH_ε), amorphous region (ΔH_A), and phase transferring (ΔH_{trans}). Thus the excess

enthalpy could be presented as the sum of the mentioned enthalpies, as Eguation (9).

$$\Delta H_{excess} = \Delta H_s + \Delta H_{GB} + \Delta H_\varepsilon + \Delta H_A + \Delta H_{trans} \quad (9)$$

A detailed information for calculating each term in Eguation (9) has been provided by Sasikumar *et al*. (2009) [38]. They calculated the stored energy for mechanically-activated ilmenite, and concluded that a major part of the energy is stored as the strain energy, structural disorder, and in defects with short relaxation times. However, our results based on long-lived defects, as shown in Table 3, indicate that contribution of the elastic strain energy to the total stored energy is negligible, and the stored energy related to the amorphization degree is more dominant.

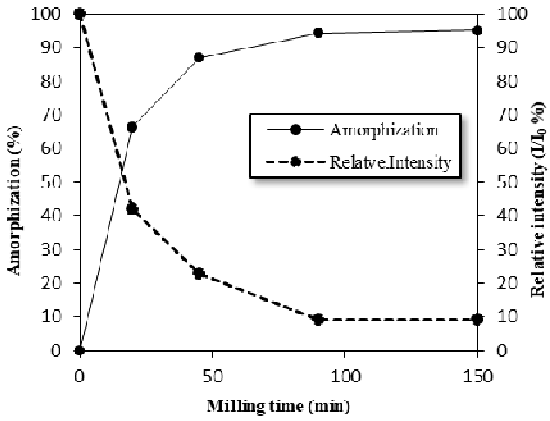

Figure 13. Change in the X-ray amorphization degree and average relative intensity (I/I_0) of ground ilmenite.

Table 3. Stored energy and its distribution.

Milling time (min)	ΔHs (j/mol)	ΔH_{GB} (J/mol)	ΔHε (J/mol)	ΔH_A (kJ/mol)	ΔH_{Excess} (kJ/mol)
0	0	0	0.00	0	0
20	44.21	65.52	0.18	49.15	49.26
45	59.53	138.12	2.78	64.04	64.24
90	66.05	381.60	7.00	70.00	70.46
150	76.71	646.21	15.21	70.75	71.48

3.6. Reactivity

In order to briefly investigate the reactivity of mechanically-activated ilmenite, the non-activated and activated samples were leached by 50% (w/w) sulfuric acid at 80 ºC for 240 min. The extraction of Ti and the weight of leach residue are shown in Figure 14. It could be seen that only 16.57% of Ti was leached from the non-activated sample, while the extraction of Ti was increased to 92.95% from the activated sample for 150 min. As the dissolution process was completed, a severe weight loss in the residue was observed. For achieving an insight to the changes in the reaction kinetic as a result of mechanical activation, the leaching kinetic tests were performed as a function of the leaching time up to 240 min. The results obtained are shown in Figure 15. As presented, the extraction rate of Ti increases significantly in the activated samples in comparison to the non-activated sample. The extraction rate at the initial stages of the leaching goes up rapidly in comparison with the extraction rate at the prolonged stages. The extraction after 35 min of leaching increased from 6.55% in the non-activated sample to 65.85% for the mechanically-activated sample for 150 min. The reactivity enhancement can be attributed to the structural changes of activated ilmenite.

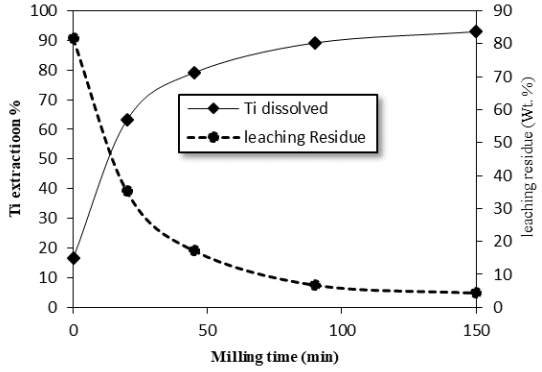

Figure 14. Variation in Ti dissolved and leaching residue as a function of milling time.

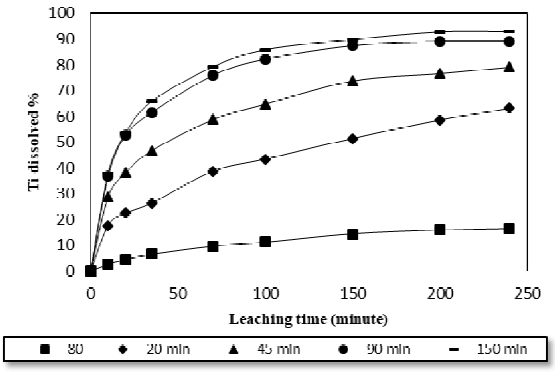

Figure 15. Effect of milling time on dissolution of ilmenite.

The semi-empirical Avrami-Erofeev (1939) equation [39] was selected to fit the dissolution data by examination of the kinetics models for the dissolution experiment data. The equation is expressed as:

$$-\ln(1-\alpha) = kt^n \quad (10)$$

where α is the fraction of Ti leached after time t, k is the rate constant, t is the reaction time, and n is a parameter representing the reaction rate control step.

The rate constant of the dissolution reaction by sulfuric acid was estimated via the kinetic experiments, as shown in Figure 16 *vs.* the milling time. It is clear that the mechanical activation significantly accelerates the leaching process, and leads to increase in the rate constant over 58 times in the mechanically-activated sample for 150 min.

Activation energy of the ilmenite dissolution reaction for the non-activated and activated sample for 150 min was estimated using the Arrhenius plots. The results obtained are depicted in Figure 17. The activation energy of 57.45 kJ/mol was calculated for un-milled ilmenite. The mechanical activation for 150 min decreases the activation energy to 41.09 kJ/mol. It can be concluded that the reactivity and leaching kinetics of ilmenite as a main process in the production of TiO_2 pigment can be improved by the mechanical activation of ilmenite due to the wide structural changes in ilmenite. However, the availability of structural characteristics at each step of the leaching process is under investigation.

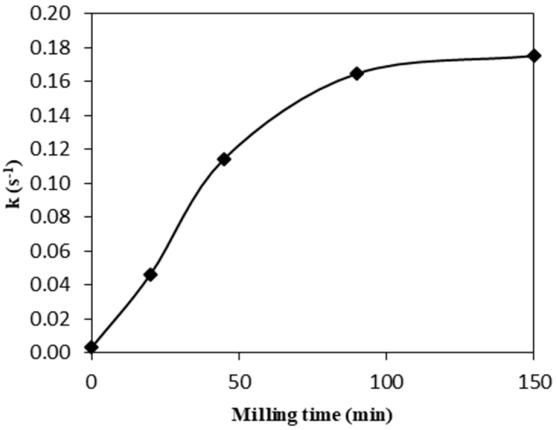

Figure 16. Influence of time of mechanical activation on the rate constant of ilmenite leaching.

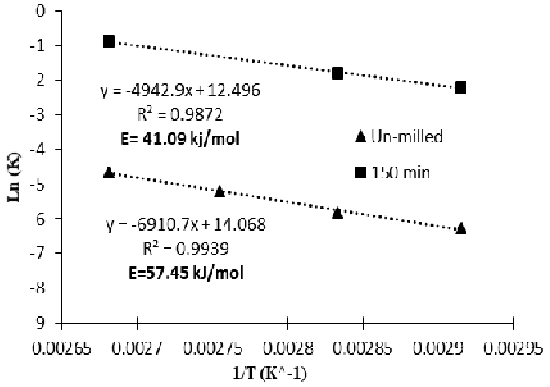

Figure 17. Arrhenius plots of un-milled and 150 min milled ilmenite.

4. Conclusions

Mechanical activation resulted in a wide range structural changes in the ilmenite structure and reactivity as follows:

1- The BET surface area was increased up to 10.76 m^2/g in the milled ilmenite for 150 min. The fine particles were agglomerated with accessible pores after 45 min of intensive dry milling.

2- As s results, it was found that the surface-weighted crystallite size was 4.45 nm after 150 min in the planetary mill corresponding to the volume-weighted crystallite size of 8 nm and 11.18 nm, obtained by the Williamson-Hall and Rietveld methods, respectively. After 150 min of mechanical activation, the root mean square strain, $< \varepsilon^2_{L=10nm} >^{1/2}$, was increased to 0.78% corresponding to the strains of 1.43% and 1.044% obtained by the Williamson-Hall and Rietveld methods, respectively.

3- A detailed analysis indicated that the role of excess grain boundary energy was dominant in comparison to the effect of excess free volume of grain boundary, so reduction of the crystallite size led to contraction of the ilmenite unit cell after 150 min.

4- After 150 min of intensive milling, the amorphization degree reached 95%, and the stored energy determination revealed that the contribution of X-ray amorphization into excess energy was dominant.

5- The rate constant of the dissolution reaction of ilmenite was increased over 58 times for the 150 min milled activated sample. Activation energy of the ilmenite dissolution reaction was decreased from 57.45 kJ/mol in the non-activated ilmenite to 41.09 kJ/mol in the activated sample for 150 min.

6- The results obtained suggest that mechanical activation would be successfully employed in the initial stage of TiO_2 pigment production, leaching, which is under investigation in our research center.

Acknowledgments

The support provided by the Mineral Processing Research Center of Sahand University of Technology is gratefully acknowledged. The authors also would like to acknowledge the Iranian Mines and Mining Industries Development and Renovation (IMIDRO) for the financial support of this research work.

References

[1]. Lin I. (1998). Implications of fine grinding in mineral processing mechanochemical approach. Journal of thermal analysis and Calorimetry. 52 (2):453-61.

[2]. Baláž P. (2000). Extractive metallurgy of activated minerals: Elsevier.

[3]. Boldyrev V., Tkáčová K (2000). Mechanochemistry of solids: past, present, and prospects. Journal of materials synthesis and processing. 8 (3-4):121-32.

[4]. Tkáčová K. (1989). Mechanical activation of minerals: Veda.

[5]. Welham N. and Llewellyn D. (1998). Mechanical enhancement of the dissolution of ilmenite. Minerals Engineering. 11 (9):827-41.

[6]. Chen Y., Williams J., Campbell S., and Wang G. (1999). Increased dissolution of ilmenite induced by high-energy ball milling. Materials Science and Engineering: A. 271 (1-2):485-90.

[7]. Li C., Liang B., Guo L-h, and Wu Z-b. (2006). Effect of mechanical activation on the dissolution of Panzhihua ilmenite. Minerals Engineering. 19 (14):1430-8.

[8]. Li C., Liang B., Wang H. (2008). Preparation of synthetic rutile by hydrochloric acid leaching of mechanically activated Panzhihua ilmenite. Hydrometallurgy. 91 (1-4):121-9.

[9]. Sasikumar C., Rao D., Srikanth S., Mukhopadhyay N., and Mehrotra S. (2007). Dissolution studies of mechanically activated Manavalakurichi ilmenite with HCl and H_2SO_4. Hydrometallurgy. 88 (1-4):154-69.

[10]. Sasikumar C., Rao D., Srikanth S., Ravikumar B., Mukhopadhyay N., and Mehrotra S. (2004). Effect of mechanical activation on the kinetics of sulfuric acid leaching of beach sand ilmenite from Orissa, India. Hydrometallurgy. 75 (1-4):189-204.

[11]. Zhang L., Hu H., Wei L., Chen Q., and Tan J. (2010). Hydrochloric acid leaching behaviour of mechanically activated Panxi ilmenite ($FeTiO_3$). Separation and Purification Technology. 73 (2):173-8.

[12]. Zhang L., Hu H., Wei L., Chen Q., and Tan J. (2010). Effects of mechanical activation on the HCl leaching behavior of titanaugite, ilmenite, and their mixtures. Metallurgical and Materials Transactions B. 41 (6):1158-65.

[13]. Pourghahramani P. and Forssberg E. (2006). Comparative study of micro-structural characteristics and stored energy of mechanically activated hematite in different grinding environments. International Journal of Mineral Processing. 79 (2):120-39.

[14]. Pourghahramani P. and Azami M.A. (2015). Mechanical activation of natural acidic igneous rocks for use in cement. International Journal of Mineral Processing. 134:82-8.

[15]. Senna M. (1989). Determination of effective surface area for the chemical reaction of fine particulate materials. Particle and Particle Systems Characterization. 6 (1-4):163-7.

[16]. Krumm S., editor WINFIT 1.2: version of November 1996 (The Erlangen geological and mineralogical software collection) of "WINFIT 1.0: a public domain program for interactive profile-analysis under WINDOWS". XIII Conference on clay mineralogy and petrology, praha; 1994.

[17]. Langford J.I. and Wilson A. (1978). Scherrer after sixty years: a survey and some new results in the determination of crystallite size. Journal of Applied Crystallography. 11 (2):102-13.

[18]. Pourghahramani P. and Forssberg E. (2006). Micro-structure characterization of mechanically activated hematite using XRD line broadening. International Journal of Mineral Processing. 79(2):106-19.

[19]. Warren B.E. (1969). X-ray Diffraction: Courier Corporation.

[20]. Bourniquel B., Sprauel J., Feron J., and Lebrun J., editors. (1989). Warren-Averbach Analysis of X-ray Line Profile (even truncated) Assuming a Voigt-like Profile. International Conference on Residual Stresses. Springer.

[21]. Rietveld H. (1969). A profile refinement method for nuclear and magnetic structures. Journal of applied Crystallography. 2 (2):65-71.

[22]. Young R. Editor. (1993). The Rietveld Method. Oxford University Press.

[23]. T. Degen MS, E. Bron, U. König, G. Nénert. (2014). The High-score suite. Powder Diffraction Volume 29 (Supplement S2):S13-S8.

[24]. Pourghahramani P. and Akhgar B. (2015). Characterization of structural changes of mechanically activated natural pyrite using XRD line profile analysis. International Journal of Mineral Processing. 134:23-8.

[25]. Li J. and Hitch M. (2016). Characterization of the micro-structure of mechanically-activated olivine using X-ray diffraction pattern analysis. Minerals Engineering. 86:24-33.

[26]. Balzar D. (1999). Voigt-function model in diffraction line-broadening analysis. International union

of crystallography monographs on crystallography. 10:94-126.

[27]. Suryanarayana C, Norton MG. (1998). X-ray diffraction: a practical approach.. New York, Plenum Publishing Corporation.

[28]. Holland T. and Redfern S. (1997). Unit cell refinement from powder diffraction data: the use of regression diagnostics. Mineralogical Magazine. 61 (1):65-77.

[29]. Schubert E.F. (2015). Doping in III-V semi-conductors: E. Fred Schubert.

[30]. Kumar R., Bakshi S., Joardar J., Parida S., Raja V., and Singh Raman R. (2017). Structural Evolution during Milling, Annealing, and Rapid Consolidation of Nano-crystalline Fe–10Cr–3Al Powder. Materials. 10 (3):272.

[31]. Qin W., Nagase T., Umakoshi Y., and Szpunar J. (2007). Lattice distortion and its effects on physical properties of nanostructured materials. Journal of Physics: Condensed Matter. 19 (23):236217.

[32]. Cammarata R.C. and Sieradzki K. (1994). Surface and interface stresses. Annual Review of Materials Science. 24 (1):215-34.

[33]. Nazarov A., Romanov A., and Valiev R. (1996). Random disclination ensembles in ultrafine-grained materials produced by severe plastic deformation. Scripta materialia. 34 (5):729-34.

[34]. Tromans D. and Meech J. (2001). Enhanced dissolution of minerals: stored energy, amorphism and mechanical activation. Minerals Engineering. 14 (11):1359-77.

[35]. Wagner M. (1992). Structure and thermodynamic properties of nano-crystalline metals. Physical Review B. 45 (2):635.

[36]. Chattopadhyay P., Nambissan P., Pabi S., and Manna I. (2001). Polymorphic bcc to fcc transformation of nano-crystalline niobium studied by positron annihilation. Physical Review B. 63 (5):054107.

[37]. Ohlberg S. and Strickler D. (1962). Determination of percent crystallinity of partly devitrified glass by X-ray diffraction. Journal of the American Ceramic Society. 45(4):170-1.

[38]. Sasikumar C., Srikanth S., Mukhopadhyay N., and Mehrotra S. (2009). Energetics of mechanical activation–Application to ilmenite. Minerals Engineering. 22 (6):572-4.

[39]. Avrami M. (1939). Kinetics of phase change 1. J Chem Phy. 7:1103.

تعیین مشخصات تغییرات ریزساختاری ایلمنیت در اثر فعال‌سازی مکانیکی

حسین عبادی[۱]، پرویز پورقهرمانی[۱*] و بهزاد نعمتی اخگر[۲]

۱- دانشکده مهندسی، دانشگاه صنعتی سهند تبریز، تبریز، ایران
۲- عضو هیات علمی دانشکده مهندسی معدن، دانشگاه ارومیه

ارسال ۲۰۲۱/۰۴/۱۴ ، پذیرش ۲۰۲۱/۰۶/۰۴

* نویسنده مسئول مکاتبات: pourghahramani@sut.ac.ir

چکیده:

تغیرات ساختاری ایلمنیت در اثر فعال سازی مکانیکی در حین آسیاکاری با آسیای سیاره‌ای به صورت تابعی از زمان آسیاکاری ثبت و اندازه‌گیری شد. بیشترین اندازه سطح مخصوص (BET) بعد از ۱۵۰ دقیقه آسیاکاری برابر با ۱۰/۷۶ متر مربع بر گرم اندازه‌گیری گردید. نتایج حاصل شده نشان داد که بعد از ۴۵ دقیقه آسیاکاری پدیده آگلومرا سیون ذرات به وقوع می‌پیوندد. بعد از ۱۵۰ دقیقه آسیاکاری بیشینه مقدار آمورف شدگی برابر با ۹۵ در صد اندازه‌گیری شد و تخمین انرژی ذخیره شده در شبکه ایملنیت نشان داد که درجه آمورف شدگی بیشترین سهم را در افزایش آنتالپی ذرات ایملنیت فعال شده دارد. کوچکترین اندازه کریستالیت سایز بر مبنای میانگین سطحی بر اساس روش وارن-اورباخ برابر با ۴/۴۵ نانومتر بود که این میزان بر مبنای میانگین حجمی از روش ویلیامسون-هال و ریتولد به ترتیب برابر با ۸ و ۱۱/۱۸ نانومتر تخمین زده شد. بعد از ۱۵۰ دقیقه آسیاکاری میزان تنش میانگین مربعات ($<\varepsilon^2_{L=10nm}>^{1/2}$) تا ۰/۷۸ در صد افزایش یافت که این میزان با روش ویلیامسون-هال و ریتولد به ترتیب برابر با ۱/۴۳ و ۱/۰۴ درصد محاسبه گردید. کاهش اندازه کریستالیت‌ها بعد از ۱۵۰ دقیقه فعال سازی منجر به انقباض شبکه سلول واحد ایلمنیت گردید. در اثر فعال سازی مکانیکی ایلمنیت بعد از ۱۵۰ دقیقه ثابت نرخ انحلال ایلمنیت بیش از ۵۸ برابر افزایش نشان داد و انرژی فعال‌سازی واکنش انحلال ایلمنیت از ۵۷/۴۵ کیلوژول بر مول به ۴۱/۰۹ کیلوژول بر مول کاهش یافت.

کلمات کلیدی: ایلمنیت، فعال‌سازی مکانیکی، تغییرات ساختاری، آنالیز پروفایل خطی XRD، واکنش‌پذیری.